植物生理
植物荷爾蒙

李澤民
海洋植物研究室
海洋生物科技暨資源學系

植物荷爾蒙

- Auxin
- Gibberellin
- Cytokinin
- Ethylene
- Abscisic acid

Auxin

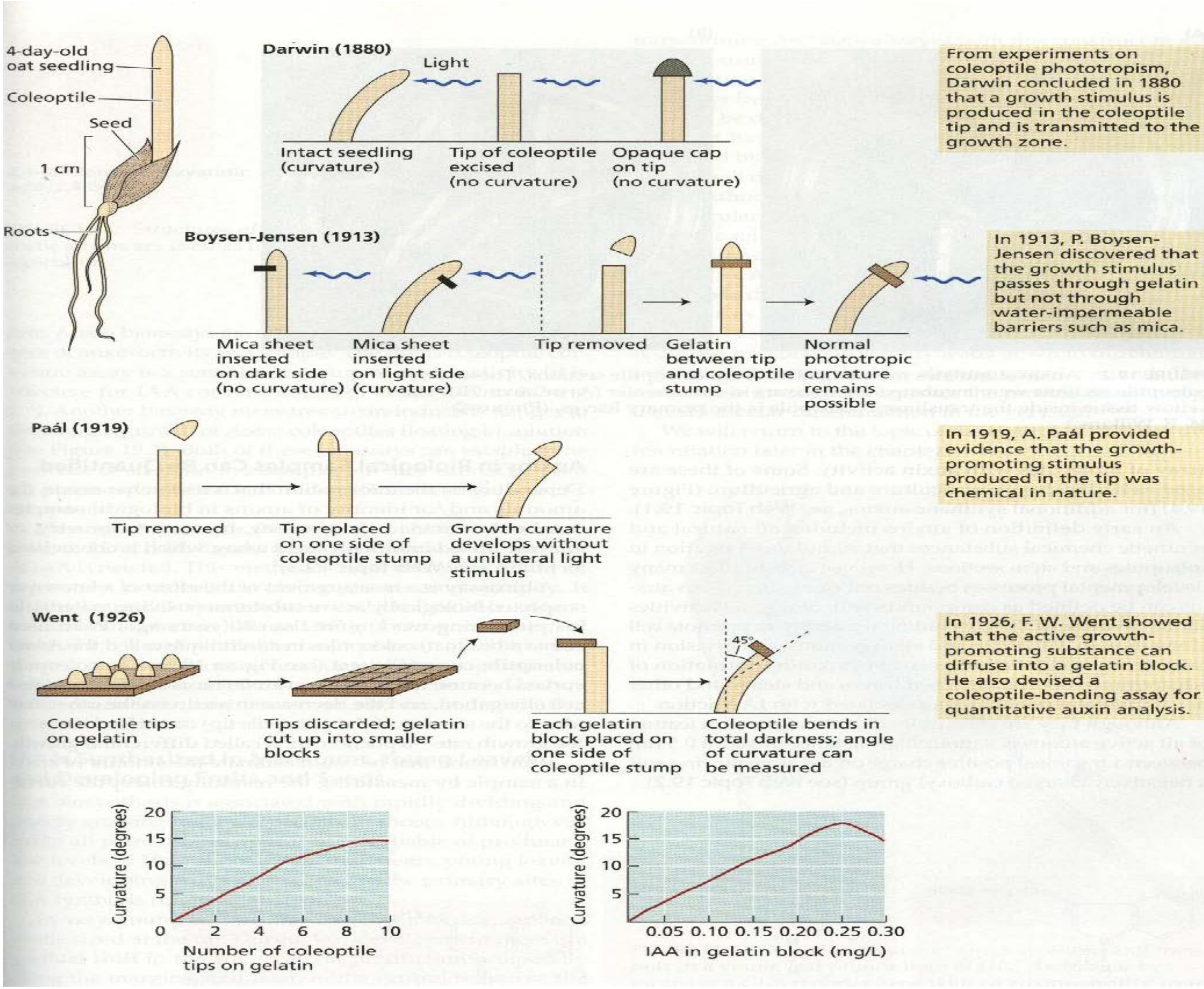

4-day-old oat seedling
Coleoptile
Seed
1 cm
Roots
Darwin (1880)
Light
Intact seedling (curvature)
Tip of coleoptile excised (no curvature)
Opaque cap on tip (no curvature)
From experiments on coleoptile phototropism, Darwin concluded in 1880 that a growth stimulus is produced in the coleoptile tip and is transmitted to the growth zone.
Boysen-Jensen (1913)
Mica sheet inserted on dark side (no curvature)
Mica sheet inserted on light side (curvature)
Tip removed
Gelatin between tip and coleoptile stump
Normal phototropic curvature remains possible
In 1913, P. Boysen-Jensen discovered that the growth stimulus passes through gelatin but not through water-impermeable barriers such as mica.
Paál (1919)
Tip removed
Tip replaced on one side of coleoptile stump
Growth curvature develops without a unilateral light stimulus
In 1919, A. Paál provided evidence that the growth-promoting stimulus produced in the tip was chemical in nature.
Went (1926)
45°
Coleoptile tips on gelatin
Tips discarded; gelatin cut up into smaller blocks
Each gelatin block placed on one side of coleoptile stump
Coleoptile bends in total darkness; angle of curvature can be measured
In 1926, F. W. Went showed that the active growth-promoting substance can diffuse into a gelatin block. He also devised a coleoptile-bending assay for quantitative auxin analysis.
Curvature (degrees)
20
15
10
5
0
2
4
6
8
10
Number of coleoptile tips on gelatin
Curvature (degrees)
20
15
10
5
0.05 0.10 0.15 0.20 0.25 0.30
IAA in gelatin block (mg/L)

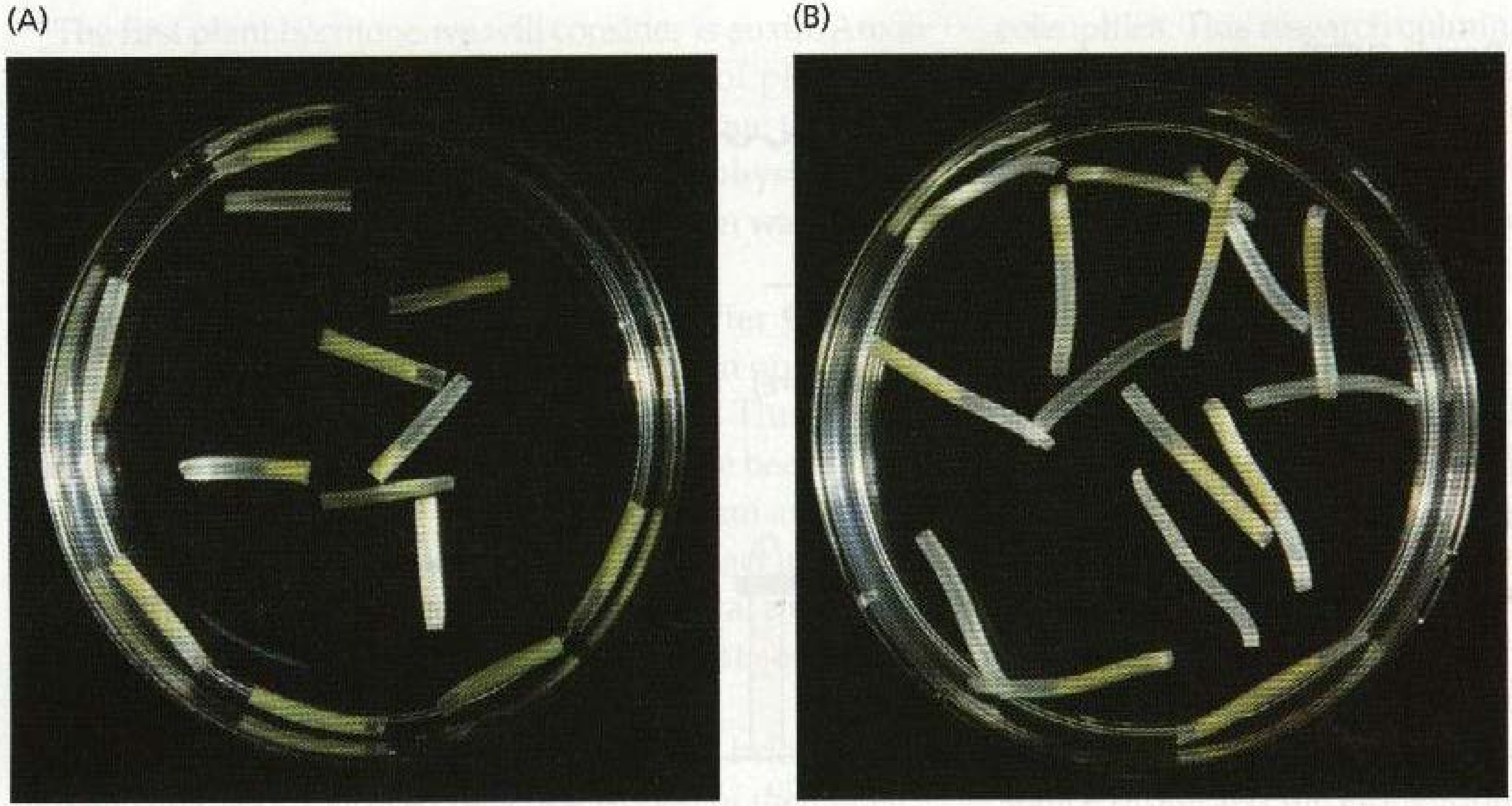

FIGURE 19.2 Auxin stimulates the elongation of oat coleoptile sections. These coleoptile sections were incubated for 18 hours in either water (A) or auxin (B). The yellow tissue inside the translucent coleoptile is the primary leaves. (Photos © M. B. Wilkins.)

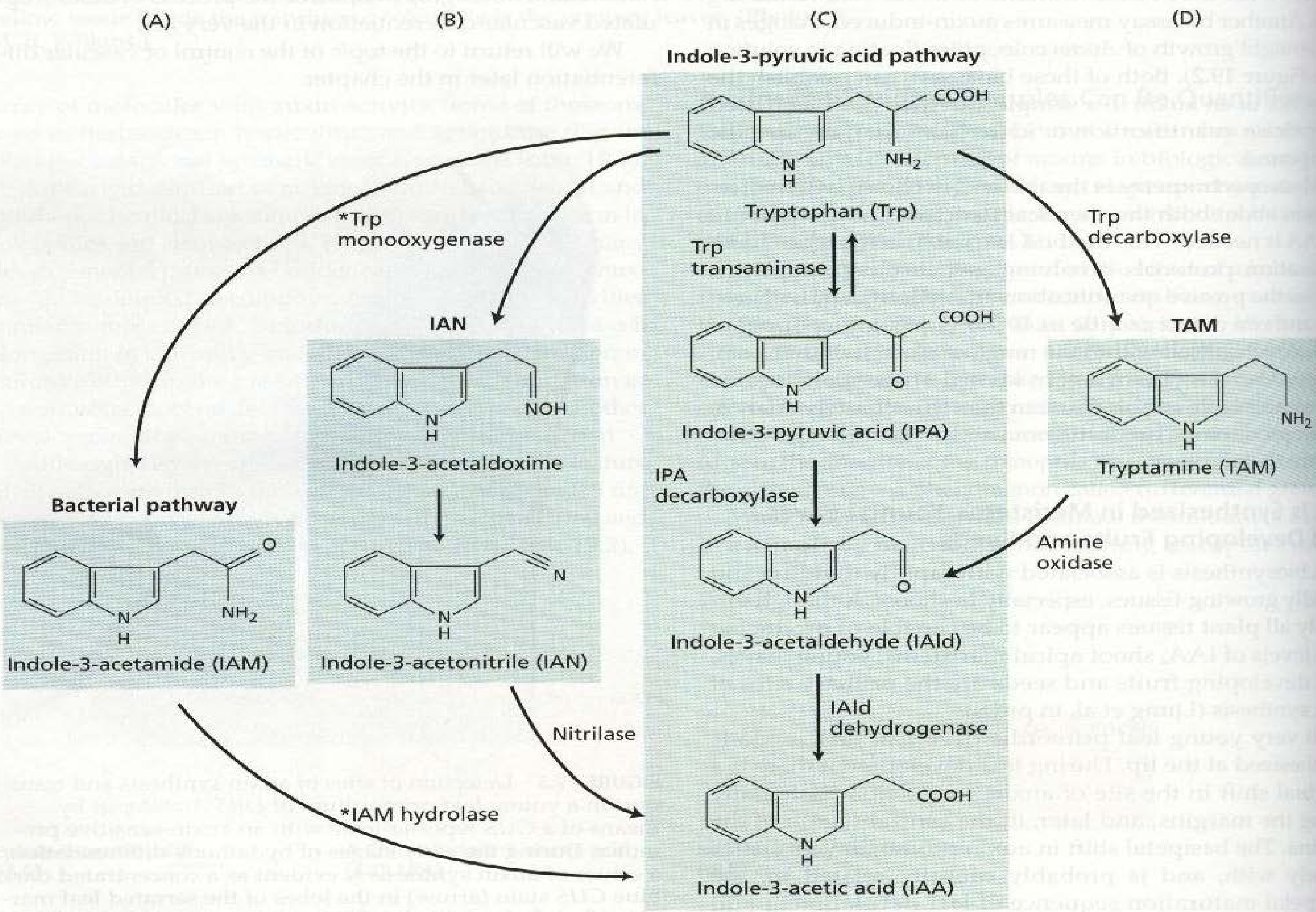

FIGURE 19.6 Tryptophan-dependent pathways of IAA biosynthesis in plants and bacteria. The enzymes that are present only in bacteria are marked with an asterisk. (After Bartel 1997.)

Acid growth theory

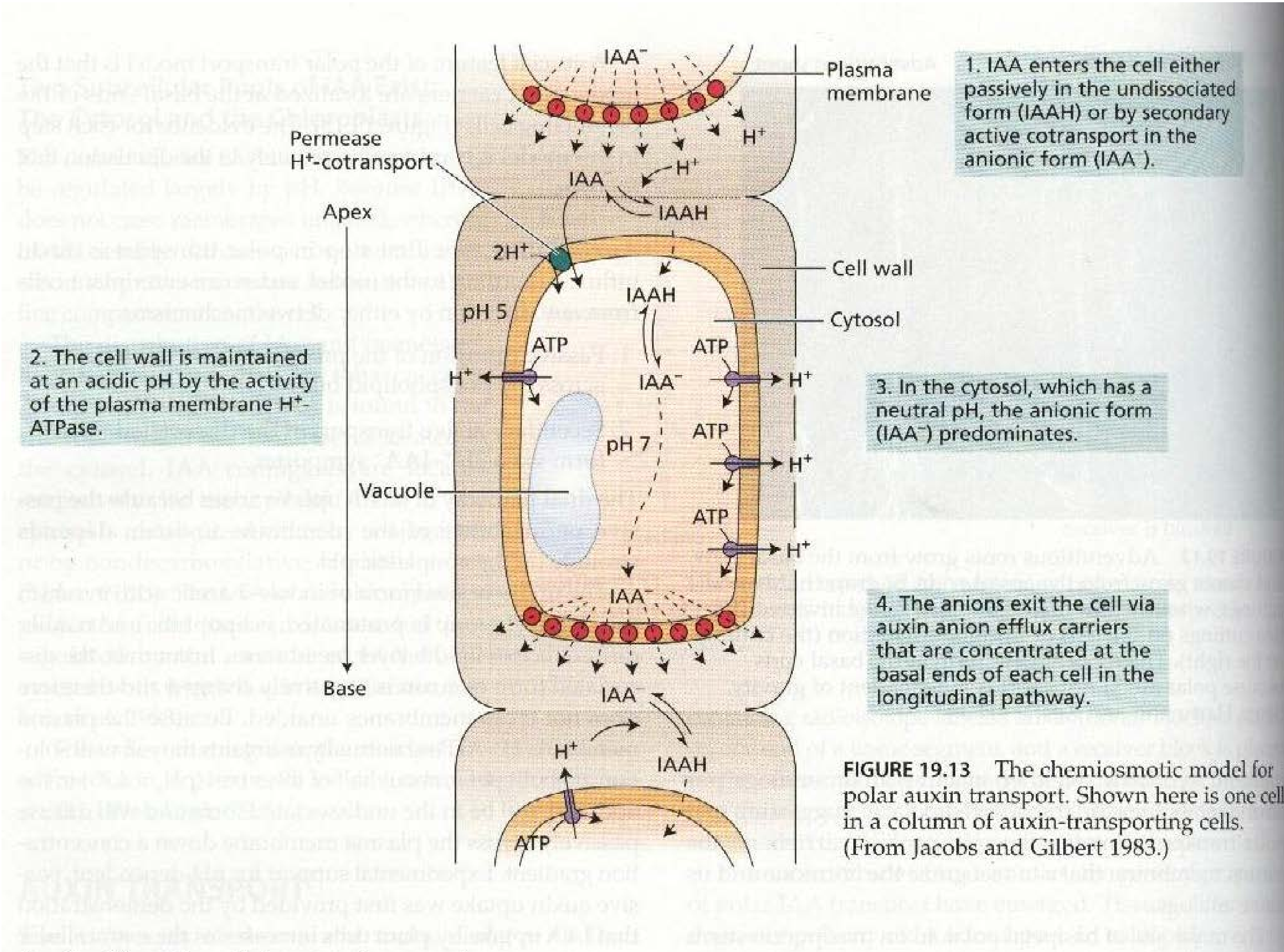

FIGURE 19.13 The chemiosmotic model for polar auxin transport. Shown here is one cell in a column of auxin-transporting cells. (From Jacobs and Gilbert 1983.)

Gibberellin

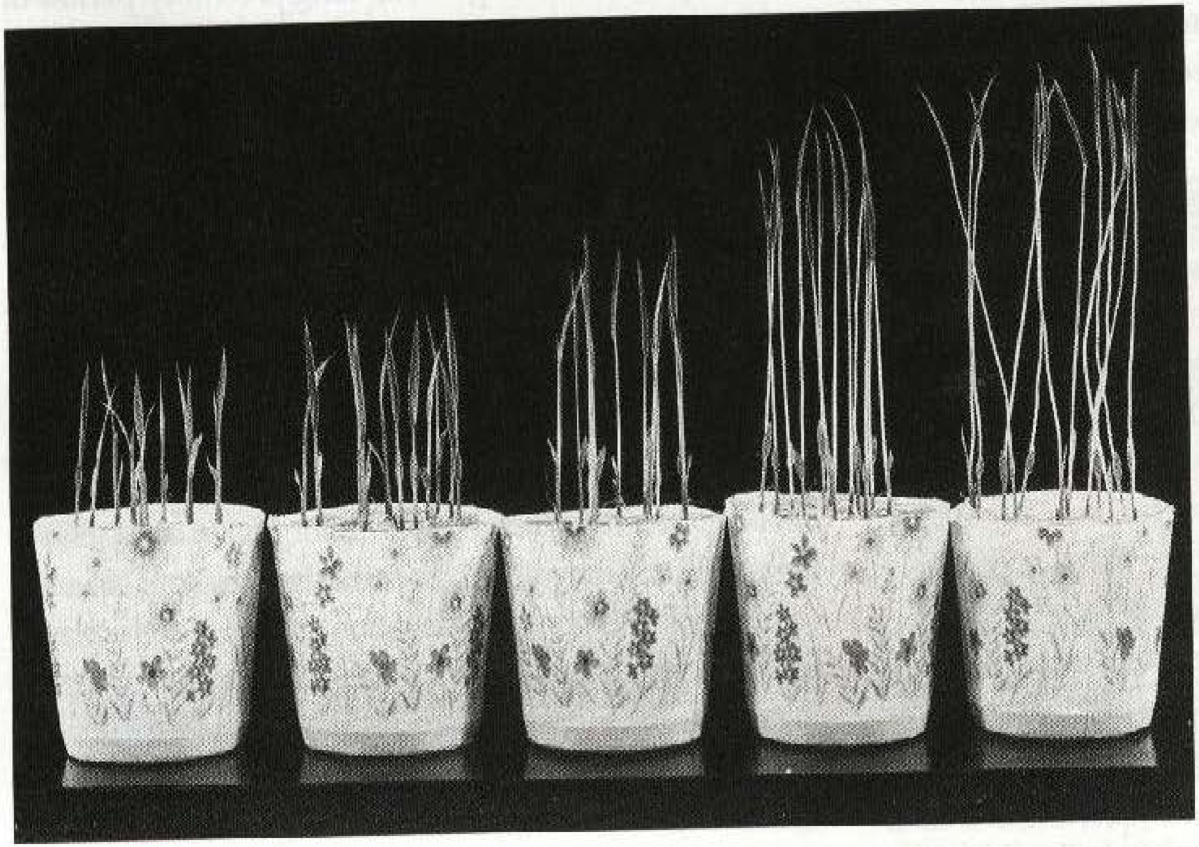

FIGURE 20.5 Gibberellin causes elongation of the leaf sheath of rice seedlings, and this response is used in the dwarf rice leaf sheath bioassay. Here 4-day-old seedlings were treated with different amounts of GA and allowed to grow for another 5 days. (Courtesy of P. Davies.)

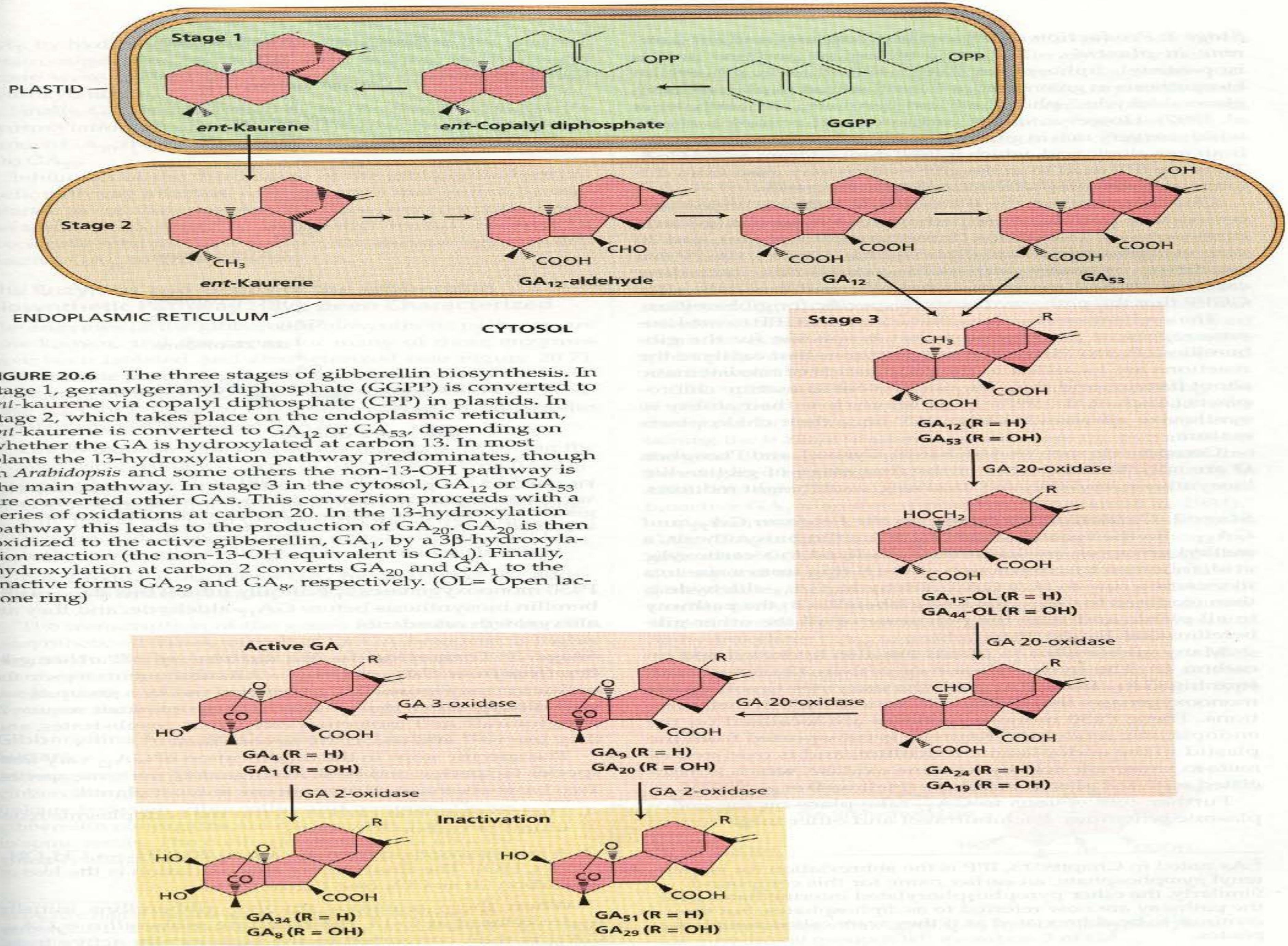

FIGURE 20.6 The three stages of gibberellin biosynthesis. In stage 1, geranylgeranyl diphosphate (GGPP) is converted to *ent*-kaurene via copalyl diphosphate (CPP) in plastids. In stage 2, which takes place on the endoplasmic reticulum, *ent*-kaurene is converted to GA_{12} or GA_{53}, depending on whether the GA is hydroxylated at carbon 13. In most plants the 13-hydroxylation pathway predominates, though in *Arabidopsis* and some others the non-13-OH pathway is the main pathway. In stage 3 in the cytosol, GA_{12} or GA_{53} are converted other GAs. This conversion proceeds with a series of oxidations at carbon 20. In the 13-hydroxylation pathway this leads to the production of GA_{20}. GA_{20} is then oxidized to the active gibberellin, GA_1, by a 3β-hydroxylation reaction (the non-13-OH equivalent is GA_4). Finally, hydroxylation at carbon 2 converts GA_{20} and GA_1 to the inactive forms GA_{29} and GA_8, respectively. (OL= Open lactone ring)

Germination aleurone layer endosperm

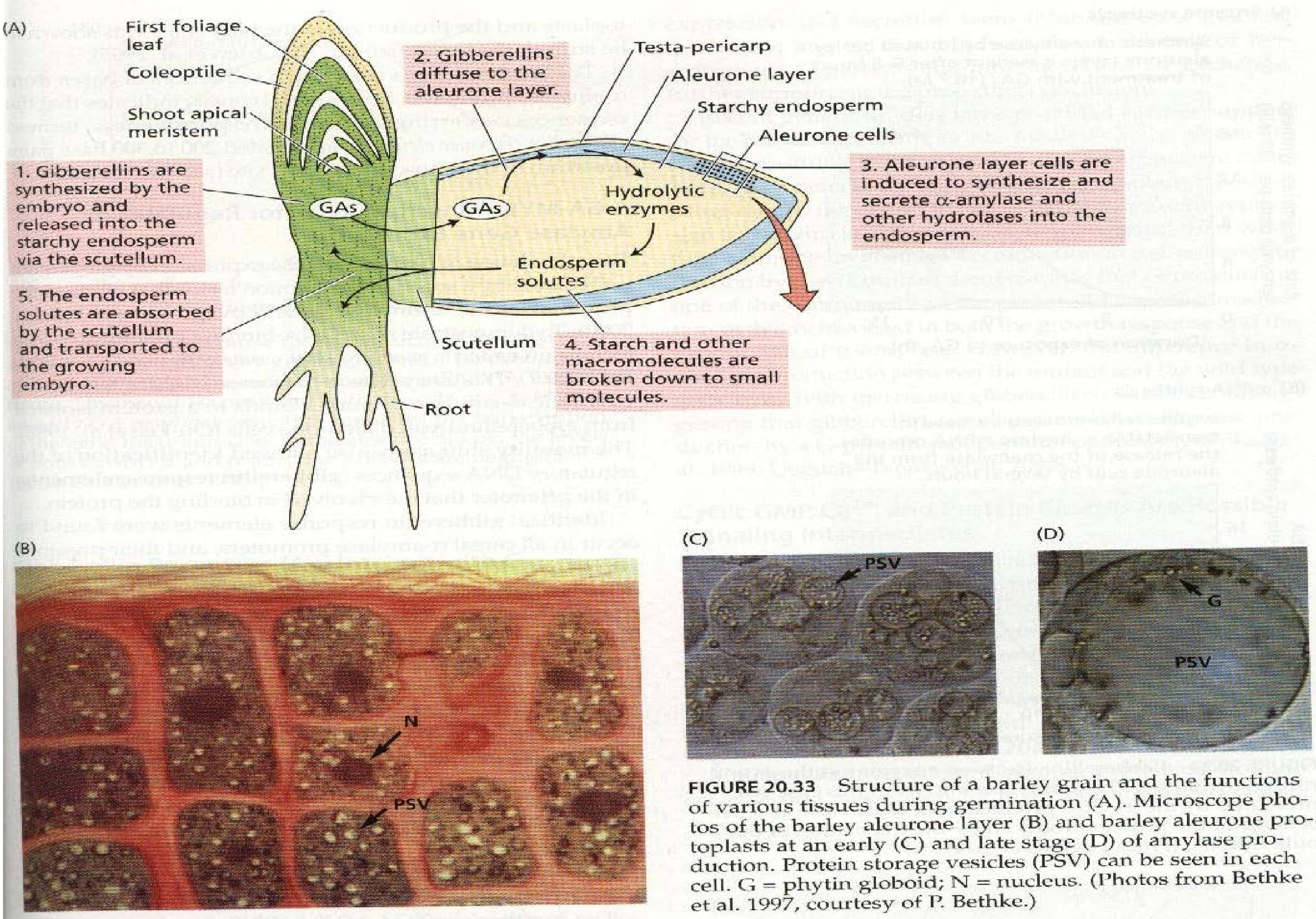

FIGURE 20.33 Structure of a barley grain and the functions of various tissues during germination (A). Microscope photos of the barley aleurone layer (B) and barley aleurone protoplasts at an early (C) and late stage (D) of amylase production. Protein storage vesicles (PSV) can be seen in each cell. G = phytin globoid; N = nucleus. (Photos from Bethke et al. 1997, courtesy of P. Bethke.)

1. GA_1 from the embryo first binds to a cell surface receptor.

2. The cell surface GA receptor complex interacts with a heterotrimeric G-protein, initiating two separate signal transduction chains.

3. A calcium-independent pathway, involving cGMP, results in the activation of a signaling intermediate.

4. The activated signaling intermediate binds to DELLA repressor proteins in the nucleus.

5. The DELLA repressors are degraded when bound to the GA signal.

6. The inactivation of the DELLA repressors allows the expression of the *MYB* gene, as well as other genes, to proceed through transcription, processing, and translation.

7. The newly synthesized MYB protein then enters the nucleus and binds to the promoter genes for α-amylase and other hydrolytic enzymes.

8. Transcription of α-amylase and other hydrolytic genes is activated.

9. α-Amylase and other hydrolases are synthesized on the rough ER.

10. Proteins are secreted via the Golgi.

11. The secretory pathway requires GA stimulation via a calcium–calmodulin-dependent signal transduction pathway.

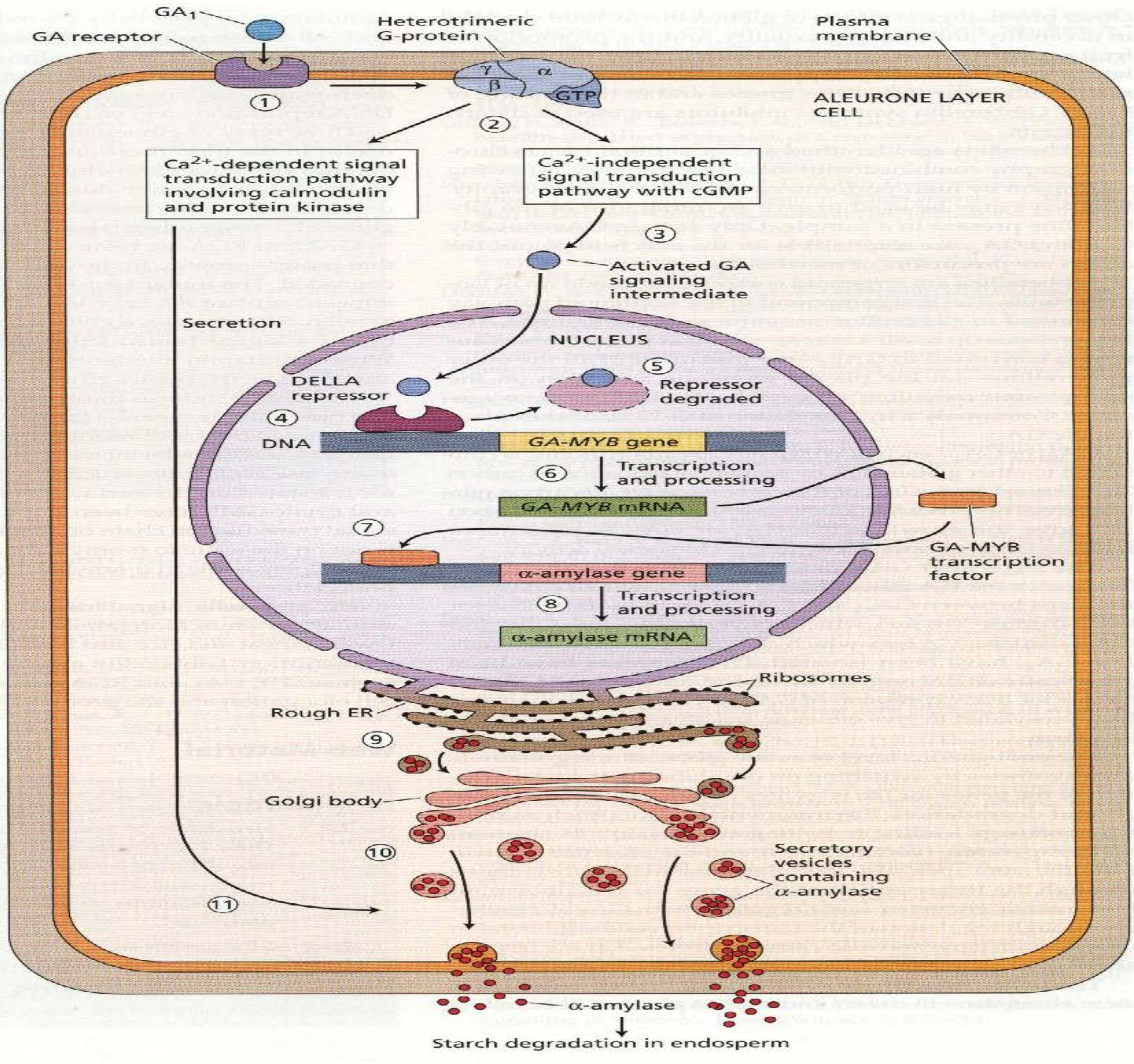

Cytokinin

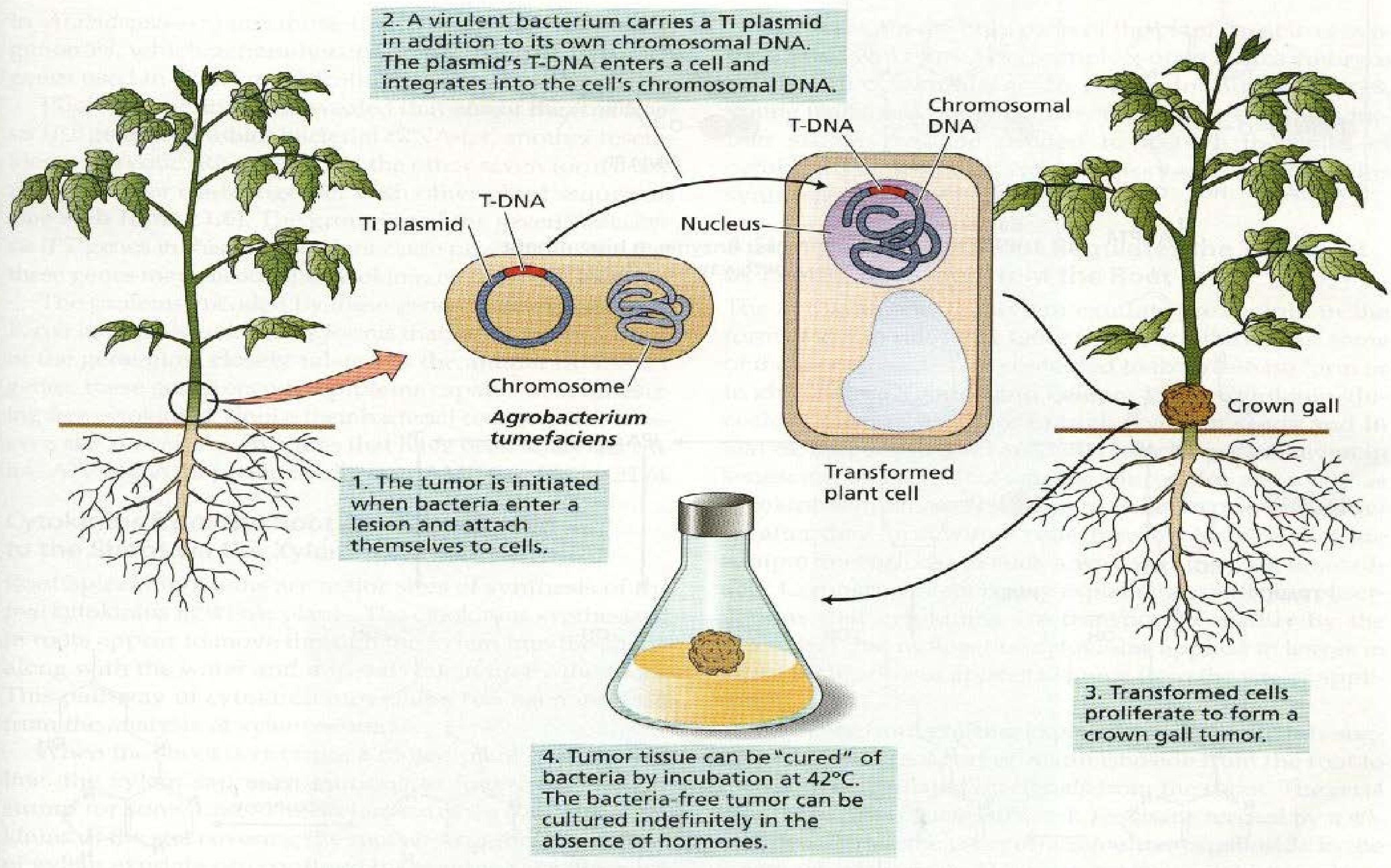

FIGURE 21.4 Tumor induction by *Agrobacterium tumefaciens.* (After Chilton 1983.)

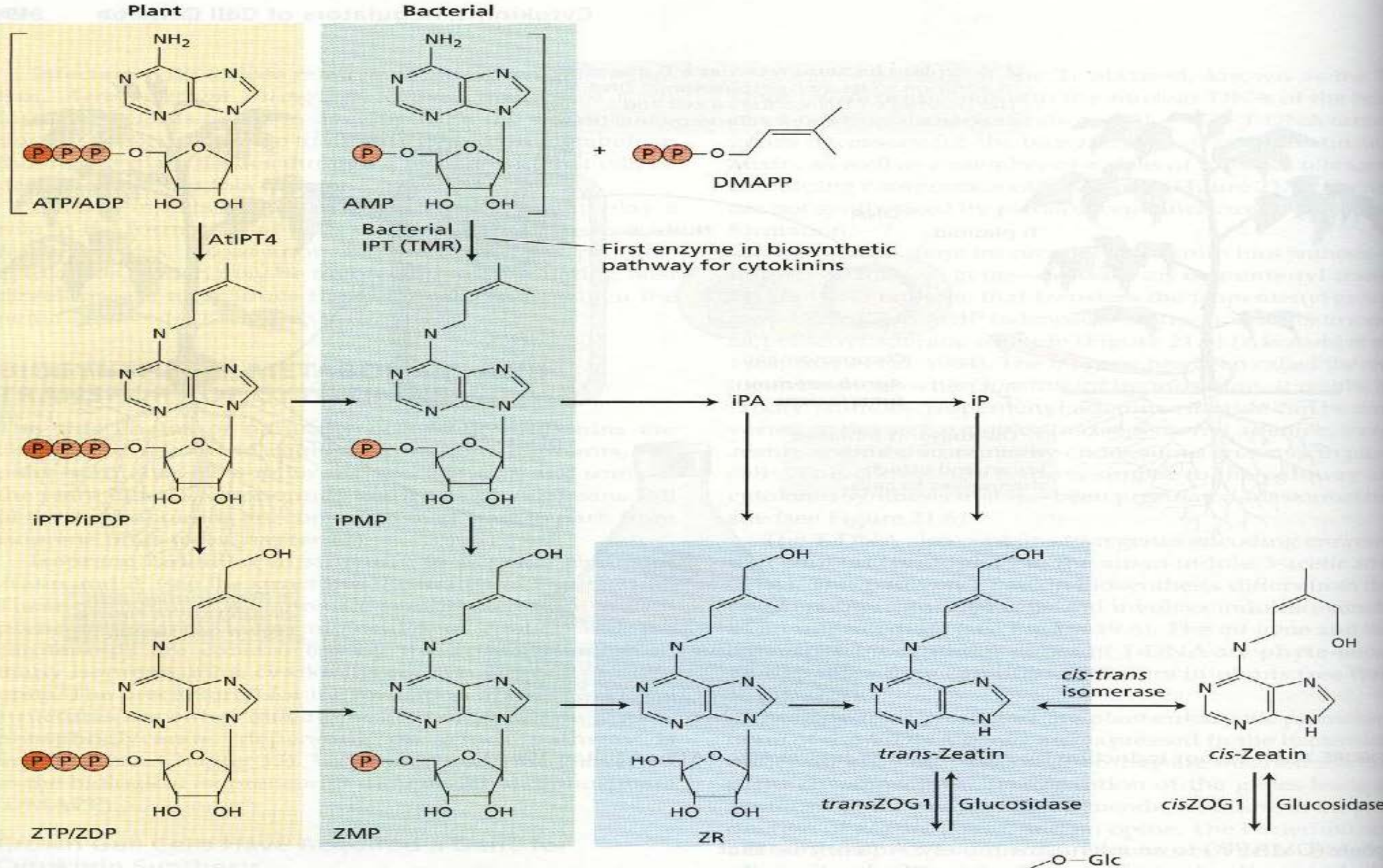

FIGURE 21.6 Biosynthetic pathway for cytokinin biosynthesis. The first committed step in cytokinin biosynthesis is the addition of the isopentenyl side chain from DMAPP to an adenosine moiety. The plant and bacterial IPT enzymes differ in the adenosine substrate used; the plant enzyme appears to utilize both ADP and ATP, and the bacterial enzyme utilizes AMP. The products of these reactions (iPMP, iPDP, or iPTP) are converted to zeatin by an unidentified hydroxylase. The various phosphorylated forms can be interconverted and free *trans*-Zeatin can be formed from the riboside by enzymes of general purine metabolism. *trans*-Zeatin can be metabolized in various ways as shown, and these reactions are catalyzed by the indicated enzymes.

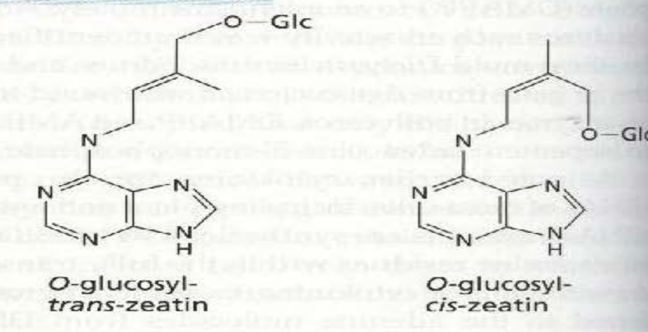

Ethylene C_2H_4

FIGURE 22.1 Ethylene biosynthetic pathway and the Yang cycle. The amino acid methionine is the precursor of ethylene. The rate-limiting step in the pathway is the conversion of AdoMet to ACC, which is catalyzed by the enzyme ACC synthase. The last step in the pathway, the conversion of ACC to ethylene, requires oxygen and is catalyzed by the enzyme ACC oxidase. The CH_3—S group of methionine is recycled via the Yang cycle and thus conserved for continued synthesis. Besides being converted to ethylene, ACC can be conjugated to *N*-malonyl ACC. AOA = aminooxyacetic acid; AVG = aminoethoxy-vinylglycine. (After McKeon et al. 1995.)

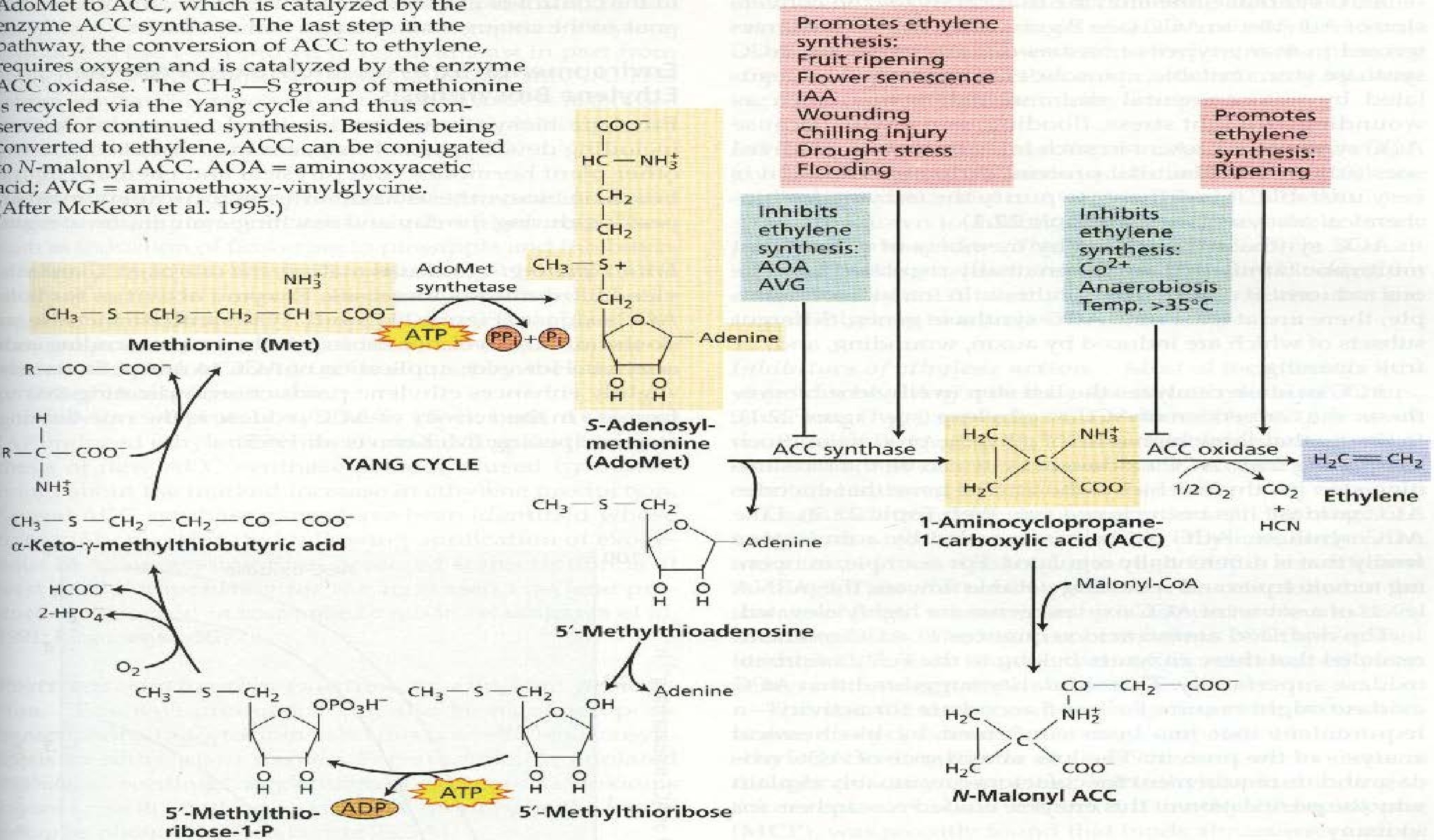

acid

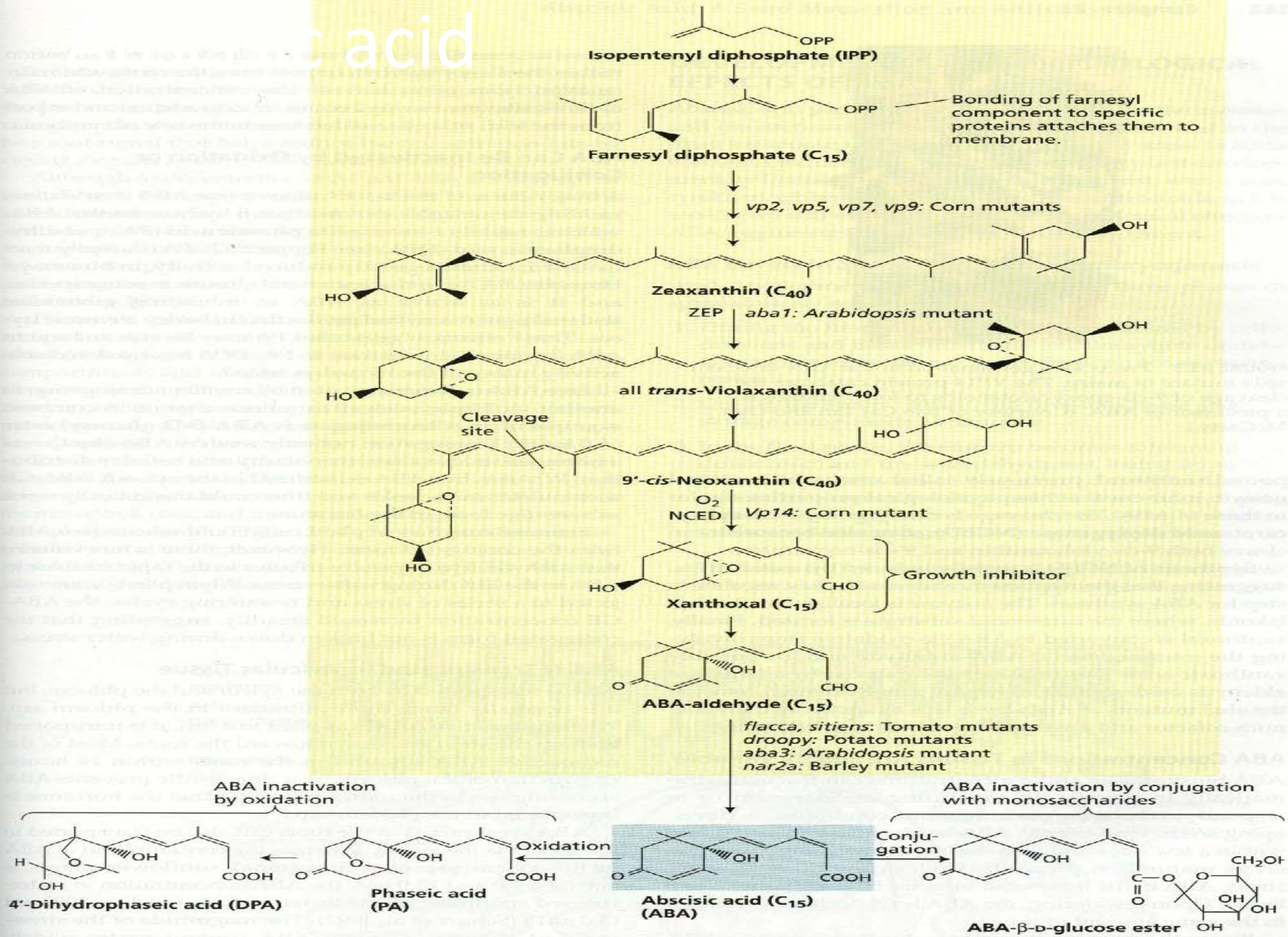

FIGURE 23.2 ABA biosynthesis and metabolism. In higher plants, ABA is synthesized via the terpenoid pathway (see Chapter 13). Some ABA-deficient mutants that have been helpful in elucidating the pathway are shown at the steps at which they are blocked. The pathways for ABA catabolism include conjugation to form ABA-β-D-glucosyl ester or oxidation to form phaseic acid and then dihydrophaseic acid. ZEP = zeaxanthin epoxidase; NCED = 9-cis-epoxy-carotenoids dioxygenase.

FIGURE 23.3 Precocious germination in the ABA-deficient *vp14* mutant of maize. The VP14 protein catalyzes the cleavage of 9-*cis*-epoxycarotenoids to form xanthoxal, a precursor of ABA. (Courtesy of Bao Cai Tan and Don McCarty.)

Stomotal opening

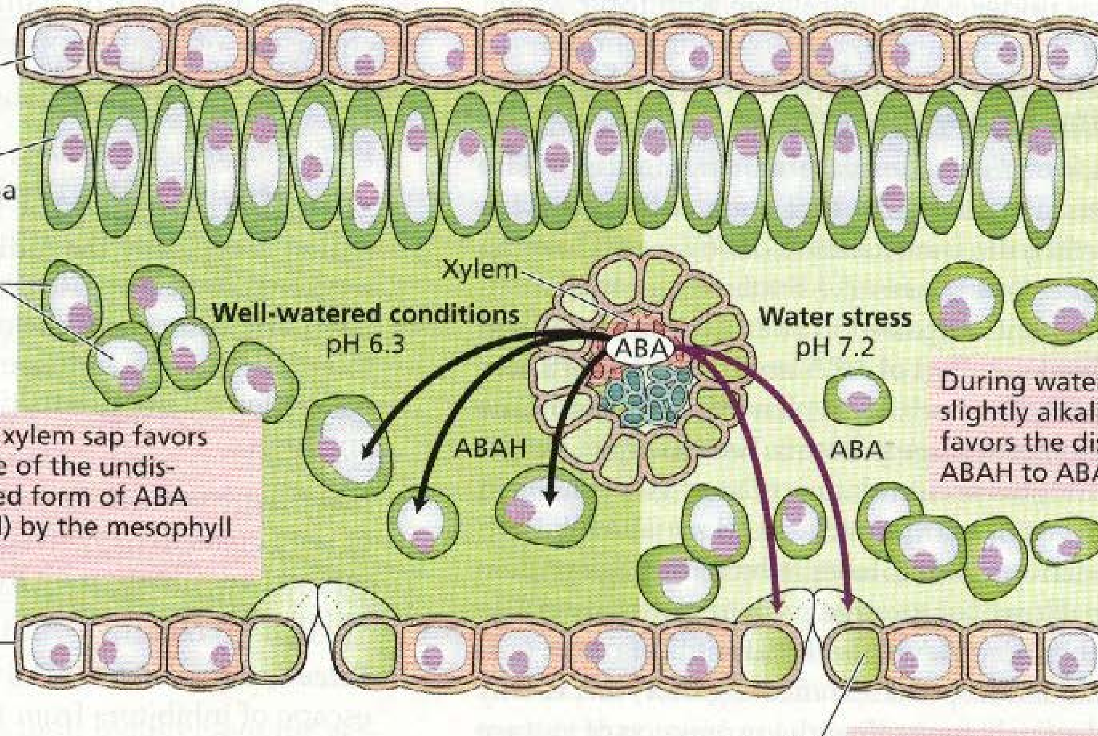

FIGURE 23.4 Redistribution of ABA in the leaf resulting from alkalinization of the xylem sap during water stress.

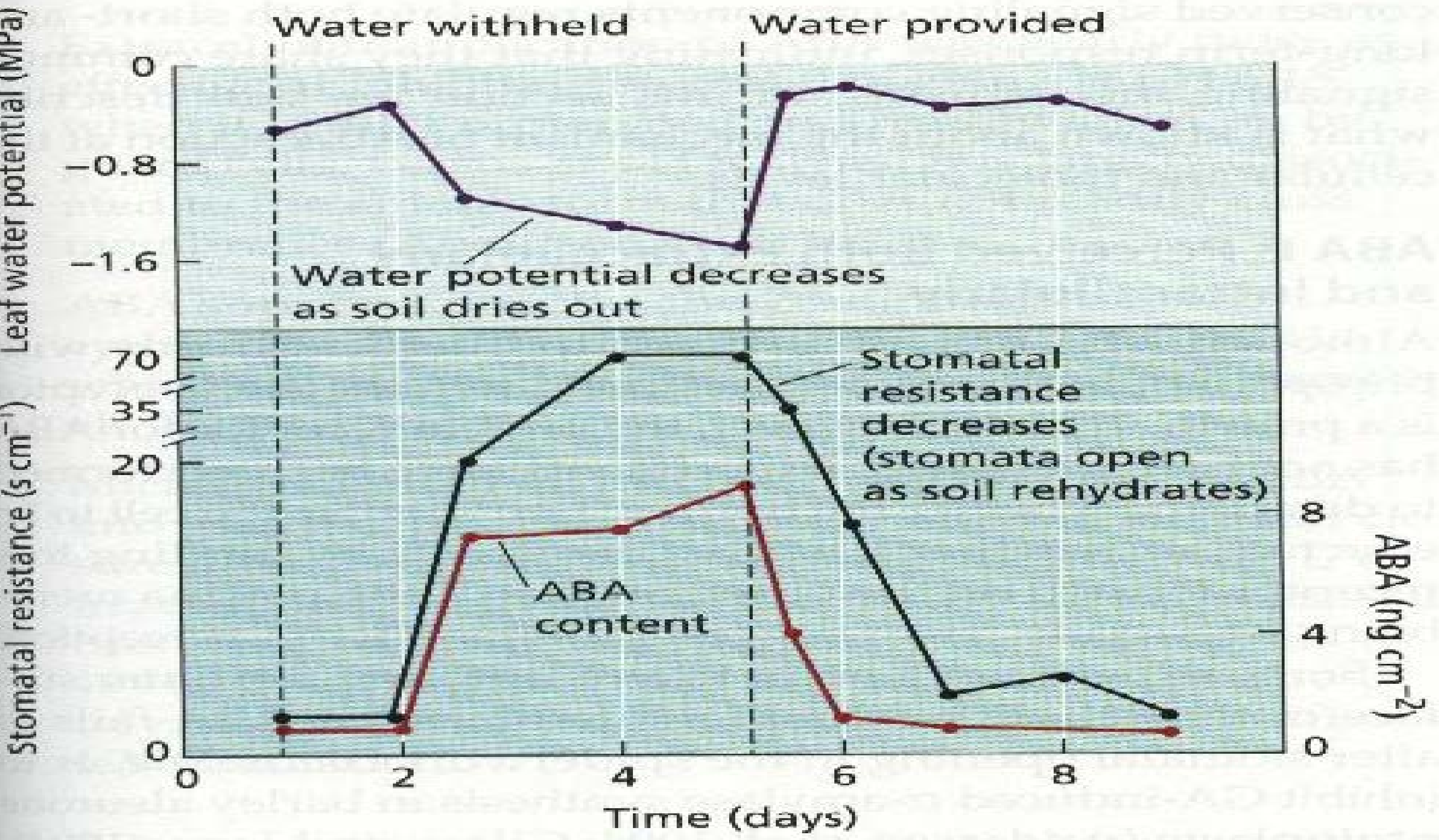

FIGURE 23.5 Changes in water potential, stomatal resistance (the inverse of stomatal conductance), and ABA content in maize in response to water stress. As the soil dried out, the water potential of the leaf decreased, and the ABA content and stomatal resistance increased. The process was reversed by rewatering. (After Beardsell and Cohen 1975.)